

# A Compact MIMO Antenna with Electromagnetic Bandgap Structure for Isolation Enhancement

Ravichandran Sanmugasundaram\*,  
Somasundaram Natarajan, and Rengasamy Rajkumar

**Abstract**—In this paper, a compact MIMO antenna with an electromagnetic bandgap structure is proposed for isolation enhancement. The proposed antenna design is coupled with an electromagnetic bandgap (EBG) structure to minimize mutual coupling between the antenna elements and to enhance the performance of the MIMO antenna configuration. The antenna is fabricated on an FR4 substrate having a dimension of  $(27.9 \times 38 \times 1.6 \text{ mm}^3)$ . The EBG structure is analyzed, and the effect on antenna performance is studied using parametric analysis. The antenna is fabricated, and the measured results are compared with simulated ones. The antenna achieves a reduction in transmission coefficient  $|S_{21}| \geq 16 \text{ dB}$  for simulated and  $|S_{21}| \geq 25 \text{ dB}$  for measured results, and attains the minimum ECC of 0.09 which is very close to the ideal value of zero and hence makes it a better choice for MIMO applications.

## 1. INTRODUCTION

Due to advancement in wireless communication technologies, a lot of devices get connected with mobile networks which demand a huge spectrum for their operation. However, the available spectrum is limited and hence requires alternative ways of effective utilization of the available spectrum. MIMO (Multiple Input Multiple Output) serves as one of the promising solutions for effective utilization of spectrum. In general, MIMO comprises a set of two or more antennas that work together to achieve increased system capacity and also mitigate the effect of multipath fading which degrades the performance of a system. In addition, the use of MIMO increases link reliability and spectral throughput of the system. Though there are significant advantages in the use of MIMO antennas, they suffer from a mutual coupling effect. This arises due to the placement of MIMO antenna elements close to each other in which the energy radiated from one antenna element can couple to other antenna elements which rigorously decreases antenna efficiency and degrades radiation pattern.

One method of reducing mutual coupling between antenna elements is by introducing decoupling elements including Electromagnetic Band Gap (EBG) structures, Meander Line Resonators, Defected Ground Structures (DGS), several shaped resonators, between the antenna elements. This significantly reduces mutual coupling by improving isolation between the antenna structures. However, the use of decoupling structures between antenna elements increases overall antenna profile which makes it bulkier and less feasible to integrate with other RF circuits. Hence a lot of researches have been carried to develop a low profile MIMO antenna with better isolation between its antenna elements. EBG structures are placed between antenna elements to suppress surface waves thereby reducing coupling between these elements. Four EBG structures [1] are embedded on a T-shaped ground stub and are placed between the radiating elements which achieve good isolation of  $-20 \text{ dB}$ . A uniplanar fractal model EBG (UPF-EBG) structure [2] is placed between two antennas separated by  $0.35\lambda_0$  distance, and a uniplanar EBG is placed

---

*Received 13 November 2020, Accepted 15 December 2020, Scheduled 22 December 2020*

\* Corresponding author: Ravichandran Sanmugasundaram (rsanmu88@gmail.com).

The authors are with the Vel Tech Rangarajan Dr. Sagunthala R&D Institute of Science and Technology, Avadi, Chennai, India.

between the circular-shaped radiating patches [3] to reduce mutual coupling. Similarly, two Minkowski fractal models with four EBG elements placed between them is realized in [4]. However, the use of the EBG structure increases the overall antenna profile. Multi-resonance EBG structures which are placed between the radiating elements separated by a gap region of  $0.42\lambda_0$  are realized in [5]. The antenna model comprises a dual substrate with a defective ground for better isolation. A double-sided EBG reduces mutual coupling in which the radiating patch is designed on the substrate achieves  $-20$  dB isolation [6]. However, it increases the fabrication complexity of the model. Mushroom type EBG structures [7] are used in the place of planar EBG structures for better isolations. Multiple mushroom-like EBG structures are used between two separated radiating patches with a distance of 30 mm to reduce mutual coupling, and the antenna radiates at 5.8 GHz frequency, and good isolation is achieved, but the EBG brings design and fabrication complexity [8]. A few simple methods are discussed to reduce the mutual coupling by employing various techniques such as the introduction of a complementary split-ring resonator (CSRR) and deployment of stub structures. However, the above designs work effectively, and they produce/work for a single resonant frequency band [9–12]. Hence, these structures are most widely used in a MIMO antenna for reducing coupling effects. A single complementary split-ring resonator (S-CSRR) between the two radiating patches of MIMO structure [13] increases its performance by reducing mutual coupling ( $|S_{12}| < -26$  dB). An average channel capacity for MIMO systems is discussed [14]. A modified split-ring resonator is used (MSRR) and placed between two orthogonal antenna elements to have better isolation,  $> 23$  dB, in [15]. A parallel-coupled line resonator is used between two antenna elements and achieves the coupling isolation of 26.2 dB [16]. Recently, a meander line resonator is placed between the radiating patches [17, 18] to reduce the mutual coupling between the elements. Though these methods achieve 8 to 10 dB isolation, the vertical feeding method brings complications of fixing with other components. Similarly, a strip line-shaped structure is designed and is etched from the ground plane [19]. It is placed in between two radiating patches for reducing mutual coupling between the radiating patches and achieves isolation of  $|S_{12}| < -20$  dB.

In order to decouple microstrip antenna elements, a DGS structure is embedded on ground plane around radiating elements [20], thereby increasing the isolation between the radiating elements. However, the area utilization to embedded DGS is high, and the probe feeding brings complexity in fabrication. A meander line with DGS method is used in intermediate position in the substrate to bring down the coupling effect which brings complication in fabrication and implementation compared to the proposed structure [21]. The use of a planar parasitic resonator reduces mutual coupling, increases structure thickness, and hence brings complexity in implementation and fabrication [22]. Polarization conversation isolator (PCI) is implemented in between the radiating elements to reduce mutual coupling, but the space required by the PCI is almost equal to the radiating element. The model is restricted only with two radiating patches, and probe feeding is applied [23].

This paper presents  $1 \times 2$  and  $2 \times 2$  MIMO structures with a novel EBG structure to minimize mutual coupling between antenna elements and to enhance the performance of the MIMO antenna configuration. The dimensions of the EBG structure are analyzed, and the effect on antenna performance is studied using parametric analysis on the dimension of EBG structure. The optimized EBG structure is coupled with the  $2 \times 2$  antenna element, and its performance is compared with other traditional antennas.

## 2. DESIGN AND ANALYSIS OF EBG STRUCTURE

The EBG structure is designed on an FR4 substrate with a relative permittivity of  $\epsilon_r = 4.4$  and dielectric loss tangent of 0.02 and has a substrate thickness of 1.6 mm. The structure is modelled using ANSYS High Frequency Structural Simulator (HFSS). The design evolution of the EBG structure comprises five stages as shown in Figure 1. The effect of the strip length and reflection coefficient characteristics are given Figure 2. It is inferred that the increment in line length (Figures 1(a) to (e)) increases the electrical length of the EBG structure and thereby decreases the resonating frequency of the EBG structure. EBG is formed using thin lines which work as an inductor, and frequency shift happens due to the increase in the line concentration. To change frequency, the line lengths are modified to resonate at desired operating frequency by progressively increasing length of the strip as shown in Figures 1(a)–(e). This shifts operating frequency towards lower band, when there is an increase in line length.

The final model is optimized to operate at 2.45 GHz with the good result of  $-27$  dB reduction in

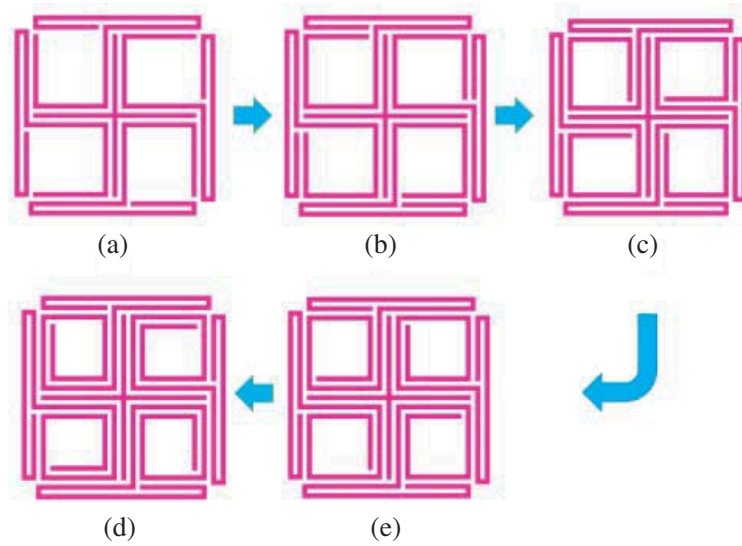


Figure 1. Evolution of formation of proposed EBG structure.

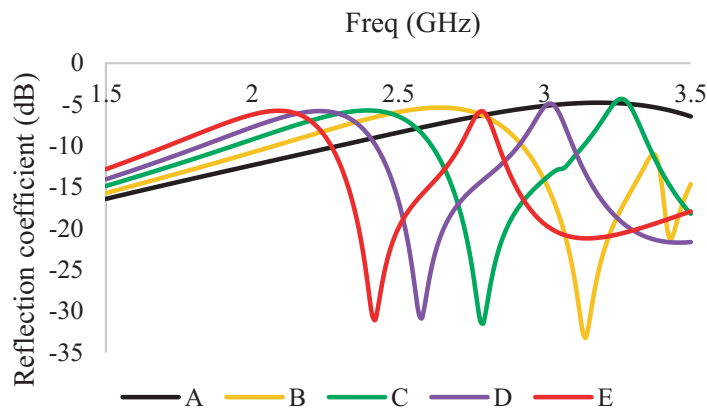


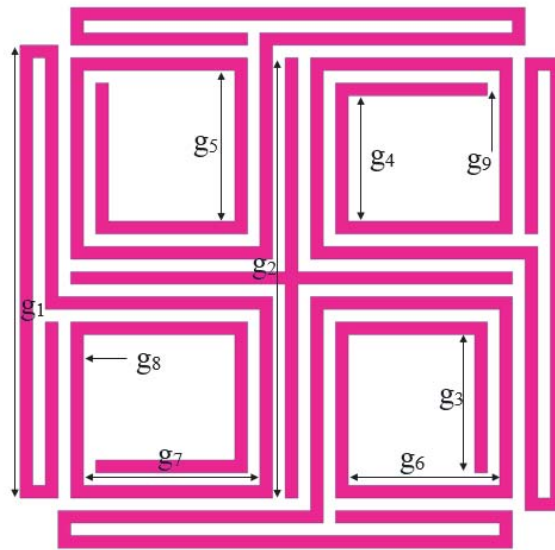
Figure 2. Effect of length of line over impedance characteristics of the antenna.

Table 1. Dimensions of the proposed EBG structure.

Parameter	Size (in mm)	Parameter	Size (in mm)
$g_1$	7.2	$g_6$	2.4
$g_2$	7	$g_7$	2.8
$g_3$	2.2	$g_8$	0.2
$g_4$	2	$g_9$	0.2
$g_5$	2.4		

mutual coupling. Based on the parametric analysis of line length, the optimized dimension of the EBG structure is given in Table 1, and its corresponding geometry is shown in Figure 3.

The proposed EBG unit cell geometry is compact in size (8.4 mm × 8.4 mm). Geometry is arrived by placing a meander line in spiral type, and line width and gap are maintained as 0.2 mm. To obtain the preferred transmission of 2.45 GHz, line lengths are optimized, and unit cells are examined in transmission line model.



**Figure 3.** Proposed EBG structure.

In order to decrease mutual coupling and to enhance the isolation between two elements, the EBG structures are connected in series as shown in Figure 4. The series of EBG structures are terminated with 50-ohm impedance and are analyzed over the entire operating band.

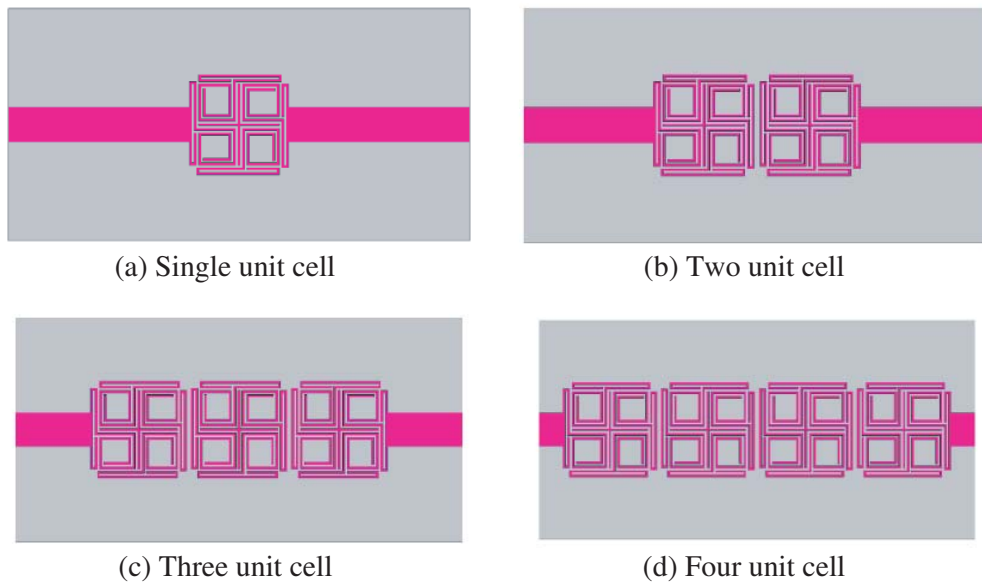


**Figure 4.** Transmission line analysis of EBG structure. (a) Single EBG structure. (b) Two EBG structure. (c) Three EBG structure. (d) Four EBG structure.

Figure 5 shows the effect of cascading EBG structures on the performance of transmission coefficient ( $S_{21}$ ). It is observed from the transmission graph that the cascading EBG structure improves isolation, thereby reducing the mutual coupling between the elements. Three unit cell EBGs are chosen to place in the proposed antenna design which gives better results than other transmission models to reduce mutual coupling.

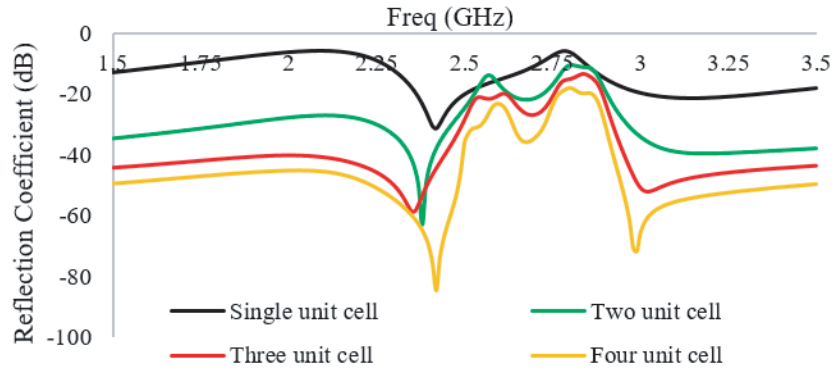


**Figure 5.** Transmission coefficient of different EBG unit cells.

### 3. ANTENNA CONFIGURATION WITH EBG STRUCTURE

A  $1 \times 2$  MIMO configured microstrip patch antenna is designed using ANSYS High Frequency Structural Simulator (HFSS) as shown in Figure 6, and the specifications are shown in Table 2. Microstrip feed is used to provide power to the radiators with the dimensions of  $27.9 \text{ mm} \times 38 \text{ mm}$  that resonates at 2.45 GHz. Radiating elements are printed on an FR4 substrate with thickness 1.6 mm, relative permittivity 4.4, and loss tangent 0.02.

**Table 2.** Dimensions of  $1 \times 2$  MIMO structure.

Parameter	Size (in mm)	Parameter	Size (in mm)
$L$	27.9	$W_1$	9
$W$	38	$W_2$	2.8
$L_1$	17	$P_g$	11
$L_2$	5		

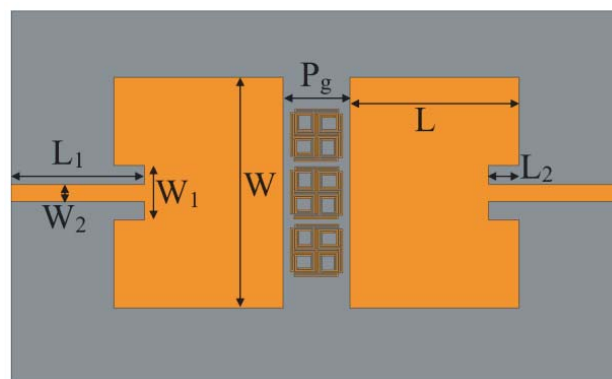


**Figure 6.**  $1 \times 2$  Proposed Structure with three EBG structures.

The geometries of different numbers of EBG structures coupled with  $1 \times 2$  MIMO structure are given in Figure 7.

Different numbers of EBG unit cells are placed between  $1 \times 2$  MIMO antenna elements, and results are analyzed. Among all, three unit cell EBG produces satisfied coupling reduction at desired frequency shown in Figure 8.

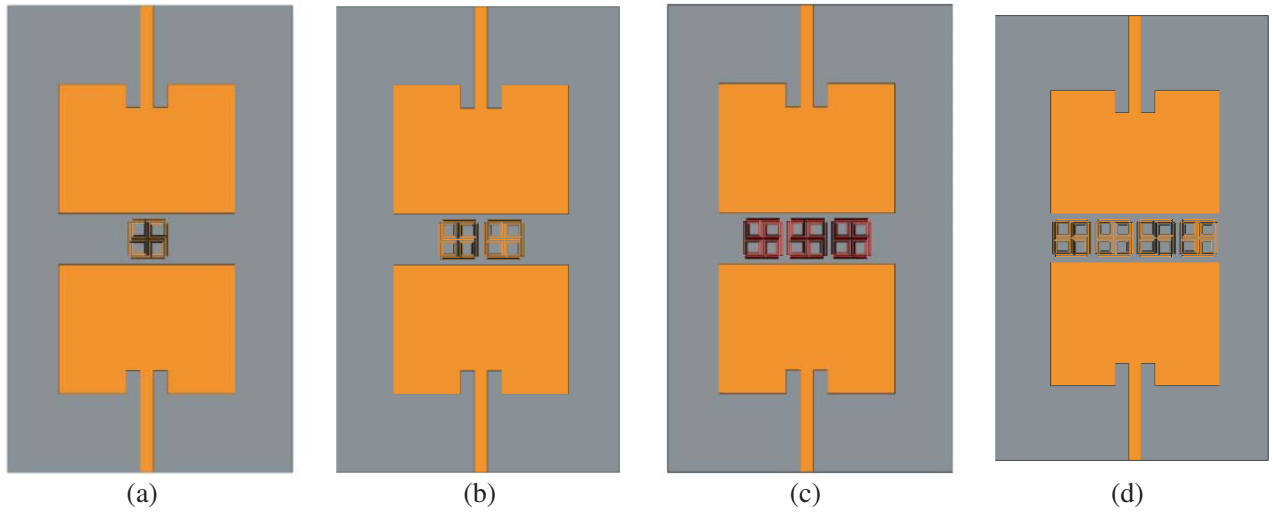


**Figure 7.** Geometry of different number of EBG structures with  $1 \times 2$  MIMO antenna. (a) Single EBG structure. (b) Two EBG structure. (c) Three EBG structure (Proposed). (d) Four EBG structure.

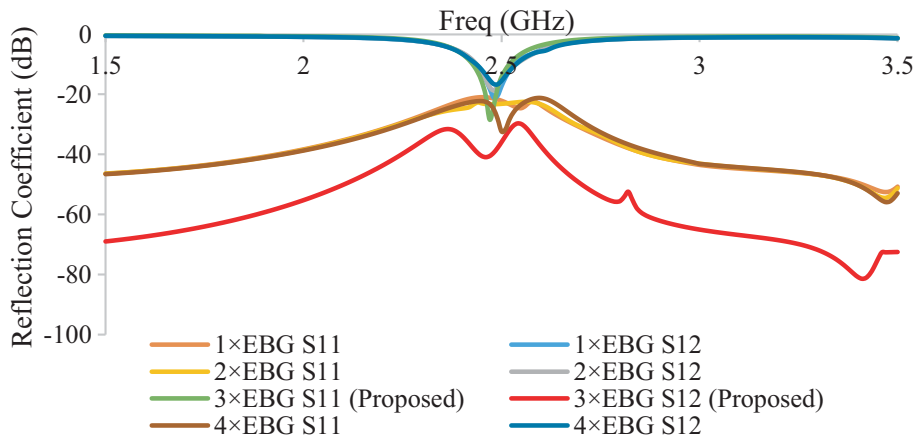


**Figure 8.** Impedance characteristics for  $1 \times 2$  antenna with EBG structure.

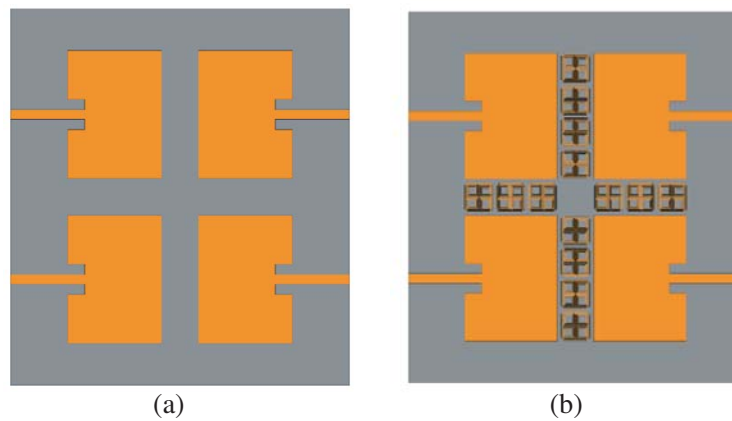


**Figure 9.**  $2 \times 2$  Proposed Structure without and with EBG. (a)  $2 \times 2$  without EBG. (b)  $2 \times 2$  with EBG.

The effect of EBG structures on  $2 \times 2$  MIMO structure is shown in Figure 9. When two ( $1 \times 2$  MIMO) radiating structures are placed near each other, MIMO mutually coupling is reduced shown in Figure 10, and this coupling is reduced directly by placing 3 EBG unit cells between two radiating patches in order to operate the structure at a desired frequency of 2.45 GHz. To place the proposed EBG structure between the two radiating patches, the edge to edge distance is adjusted as 11 mm.

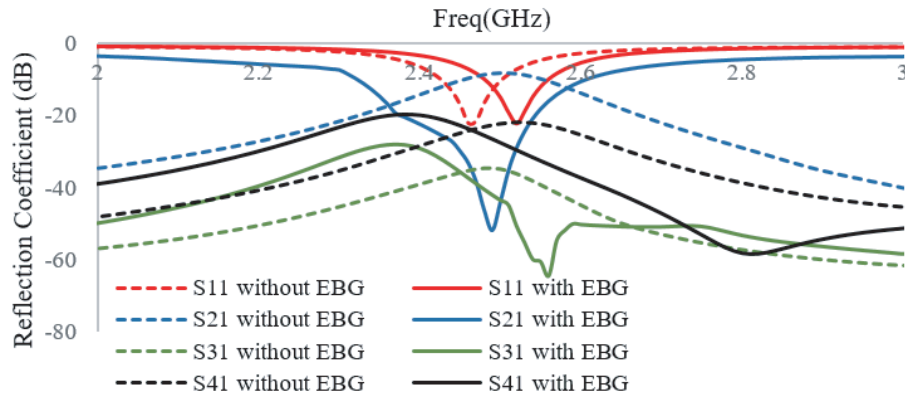


**Figure 10.** Impedance characteristics for  $2 \times 2$  antenna structure without and with EBG structure.

#### 4. RESULTS AND DISCUSSIONS

The antenna is fabricated on a low cost FR4 substrate as shown in Figure 11, and its performance characteristics are measured.

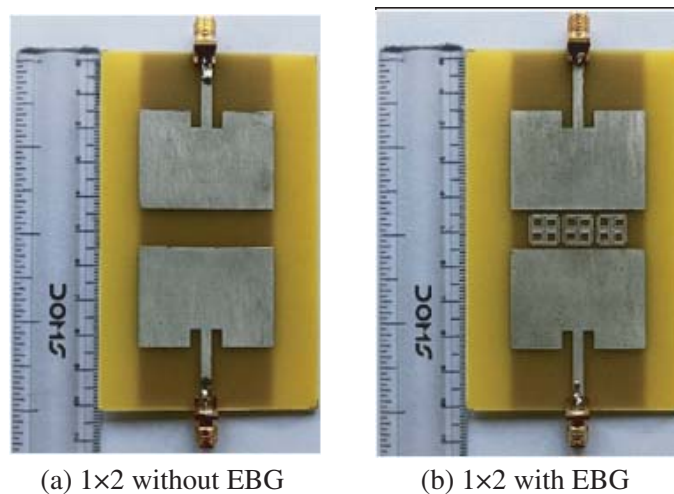


**Figure 11.** Fabricated prototype. (a)  $1 \times 2$  structure without EBG. (b)  $1 \times 2$  structure with EBG.

The simulated and measured impedance characteristics of the  $1 \times 2$  antenna structure without EBG structure are plotted and compared with the antenna structure with EBG as shown in Figure 12. It is observed that the antenna operates in the 2.4–2.5 GHz band along with  $-10$  dB reflection coefficient  $|S_{11}|$  and bandwidth of 100 MHz in the ISM band. The presence of EBG structures along with antenna elements does not alter the operating frequency much and achieves a reduction in transmission coefficient  $|S_{21}| \geq 16$  dB for simulation and  $|S_{21}| \geq 25$  dB for measurement.

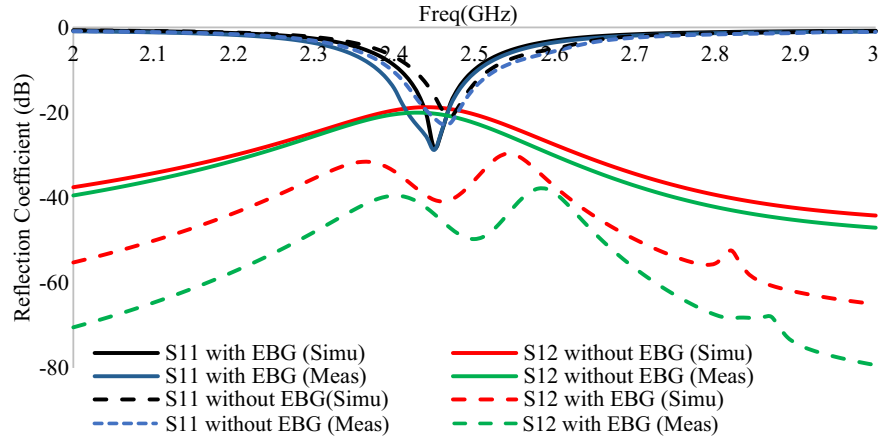


Figure 12. Impedance characteristics for  $1 \times 2$  antenna with and without EBG structure.

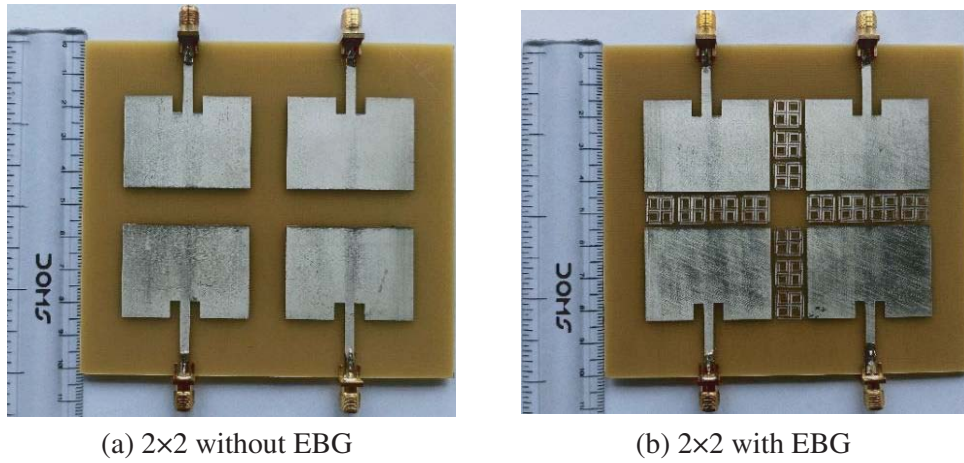


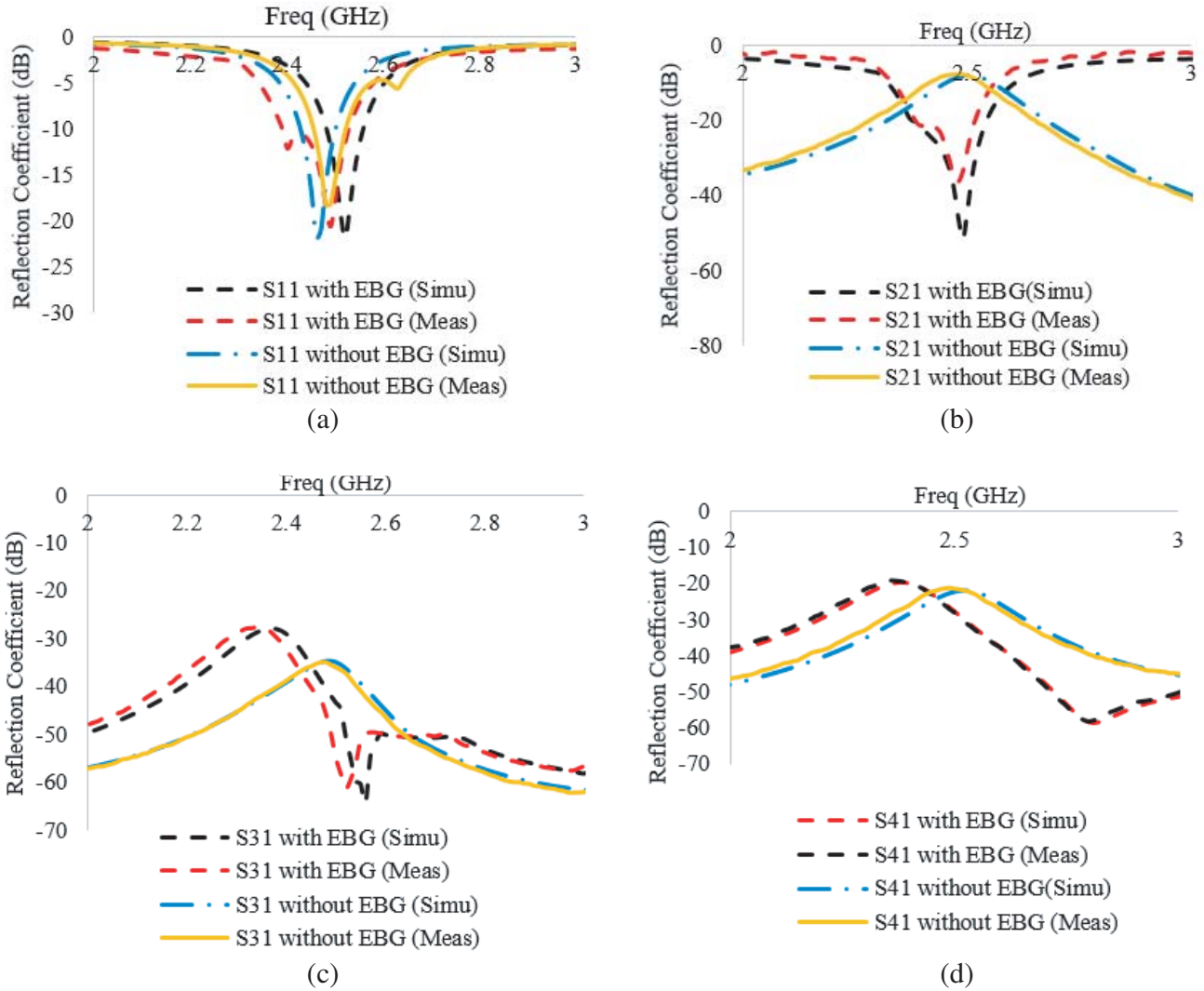
Figure 13. Fabricated prototype. (a)  $2 \times 2$  structure without EBG. (b)  $2 \times 2$  structure with EBG.

Table 3. Performance comparison of the proposed model.

Ref. No.	Size (mm <sup>3</sup> )	No. of resonators	Technique	Isolation improvement (dB)	Gain (dBi)
[1]	$50 \times 35 \times 1.6$	4	EBG	20	1.4
[2]	$68 \times 40 \times 1.6$	6	UPF-EBG	30	2
[3]	$27.2 \times 46 \times 1.6$	4	UC-EBG	18	0.5
[4]	$33.5 \times 37.5 \times 1.6$	4	EBG	22.7	5.1
[9]	$37.26 \times 28.13 \times 1.6$	5	Semi-circle CSRR	33.2	3.8
[17]	$24.8 \times 24.6 \times 1.6$	1	Meander line	8	0.2
Proposed	$27.9 \times 38 \times 1.6$	3	EBG	25	4.6

The  $2 \times 2$  antenna is fabricated and shown in Figure 13. The simulated and measured impedance characteristics of the  $2 \times 2$  antenna structure without EBG structure are plotted and compared with the antenna structure with EBG as shown in Figure 14.





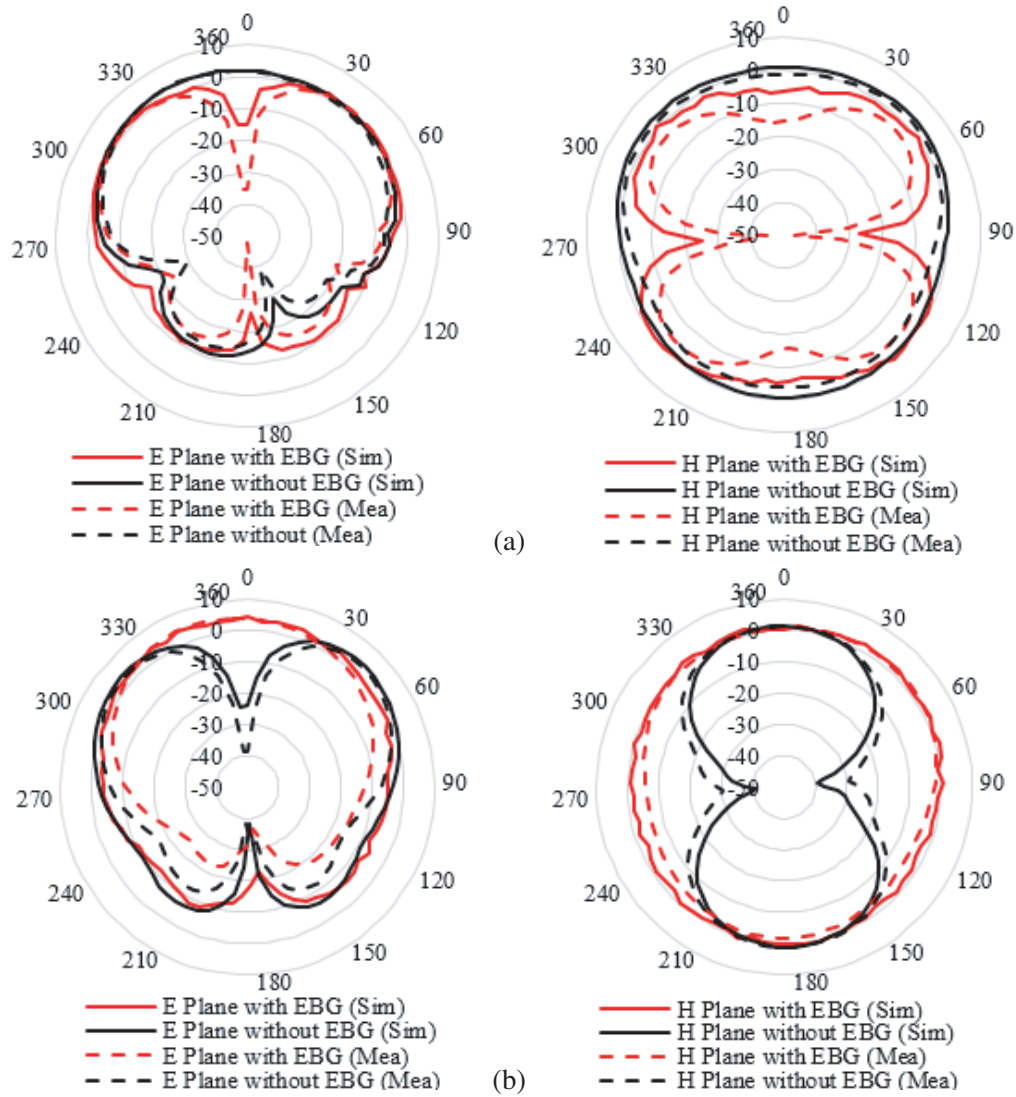
**Figure 14.** Impedance characteristics for  $2 \times 2$  antenna with and without EBG structure. (a)  $|S_{11}|$ . (b)  $|S_{21}|$ . (c)  $|S_{31}|$ . (d)  $|S_{41}|$ .

The proposed antenna has better results in terms of size, isolation, and gain than the other existing literatures which are tabulated in Table 3.

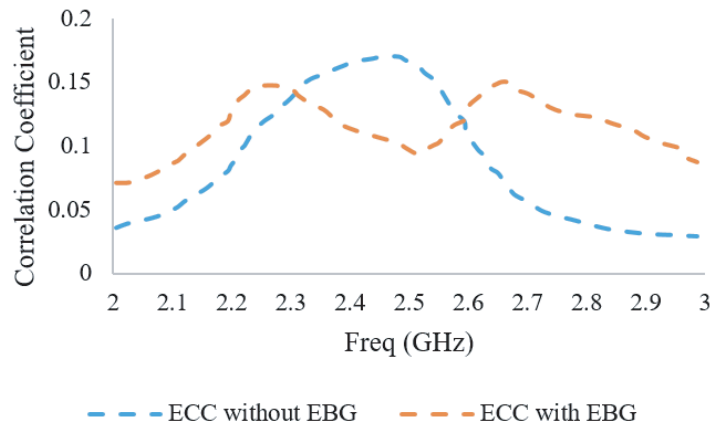
The antenna achieves a mutual coupling reduction in transmission coefficient  $\geq 25$  dB for simulation and  $\geq 20$  dB for measurement. The radiation characteristic of the antenna is measured for proposed model  $1 \times 2$  and  $2 \times 2$  antennas with and without EBG.

Figure 15 shows the radiation characteristics of the proposed model. The simulated  $E$  plane and  $H$  plane for the proposed model are compared with measured radiation characteristics for both with and without EBG structure. It is observed that the antenna gives simulated peak gain of 4.6 dBi and measured peak gain of 4.2 dBi in the direction of propagation. The antenna gives uniform omnidirectional radiation around the zenith direction. In order to analyze the isolation characteristics between antenna elements in the proposed model, envelope correlation characteristics are measured based on equation [24] given below.

$$ECC = \frac{|(S_{11}^* S_{12} + S_{21}^* S_{22})|}{(1 - |S_{11}|^2 - |S_{21}|^2) (1 - |S_{22}|^2 - |S_{12}|^2)} \quad (1)$$



**Figure 15.** Radiation characteristics of the antenna. (a)  $1 \times 2$  MIMO antenna structure Radiation pattern. (b)  $2 \times 2$  MIMO antenna structure Radiation pattern.



**Figure 16.** Envelope correlation coefficient.

Figure 16 shows envelope correlation coefficient (ECC) curves measured for the proposed model with EBG and without EBG structures which are compared. The ideal value of ECC is zero for a given model. The proposed model achieves 0.09 ECC which is very close to an ideal case. The proposed 2.45 GHz MIMO is realized using a rectangle monopole radiator because of its simple geometry.

## 5. CONCLUSION

A MIMO antenna coupled with electromagnetic band gap structures (EBGs) is proposed. The isolation characteristics of EBG structures are analyzed. The EBG structures are embedded with radiating antenna and optimized to resonate at 2.45 GHz band suitable for ISM band communications and achieve a reduction in transmission coefficient  $|S_{21}| \geq 16$  dB for simulation and  $|S_{21}| \geq 25$  dB for measurement. The antenna achieves significant impedance and gain characteristics suitable for ISM band applications. The antenna attains the minimum ECC of 0.09 which is very close to the ideal value of zero and hence makes it a better choice for MIMO applications.

## REFERENCES

1. Chen, Z., J. Hong, and Y. Deng, "Reduction of mutual coupling in UWB-MIMO antennas by using EBG structures based on a T-shaped ground branch," *2019 International Conference on Microwave and Millimeter Wave Technology (ICMMT)*, 1–3, Guangzhou, China, 2019.
2. Radhi, A. H., N. A. Aziz, R. Nilavalan, and H. S. Al-Raweshidy, "Mutual coupling reduction between two PIFA using uni-planar fractal based EBG for MIMO application," *2016 Loughborough Antennas & Propagation Conference (LAPC)*, 1–5, Loughborough, 2016.
3. Dabas, T., D. Gangwar, B. Kumar Kanaujia, and A. K. Gautam, "Mutual coupling reduction between elements of UWB MIMO antenna using small size uniplanar EBG exhibiting multiple stop bands," *AEU — International Journal of Electronics and Communications*, Vol. 93, 32–38, 2018.
4. Mohamadzade, B., A. Lalbakhsh, R. B. V. B. Simorangkir, A. Rezaee, and R. M. Hashmi, "Mutual coupling reduction in microstrip array antenna by employing cut side patches and EBG structures," *Progress In Electromagnetics Research M*, Vol. 89, 179–187, 2020.
5. Sokunbi, O., H. Attia, and S. I. Sheikh, "Microstrip antenna array with reduced mutual coupling using slotted-ring EBG structure for 5G applications," *2019 IEEE International Symposium on Antennas and Propagation and USNC-URSI Radio Science Meeting*, 1185–1186, Atlanta, GA, USA, 2019.
6. Prabhu, P. and S. Malarvizhi, "Novel double-side EBG based mutual coupling reduction for compact quad port UWB MIMO antenna," *AEU — International Journal of Electronics and Communications*, Vol. 109, 146–156, 2019.
7. Bhavarthe, P. P., S. S. Rathod, and K. T. V. Reddy, "Mutual coupling reduction in patch antenna using Electromagnetic Band Gap (EBG) structure for IoT application," *2018 International Conference on Communication Information and Computing Technology (ICCICT)*, 1–4, Mumbai, 2018.
8. Babu, K. V., B. Anuradha, and K. C. Bhushana Rao, "Reduction of mutual coupling by desegregated with EBG structure for microstrip antenna array radar applications," *2016 International Conference on Signal Processing, Communication, Power and Embedded System*, 317–320, Paralakhemundi, 2016.
9. Ambika, A. and C. Tharini, "Semicircle CSRR with circular slot array structures for high level mutual coupling reduction in MIMO antenna," *Progress In Electromagnetics Research M*, Vol. 87, 23–32, 2019.
10. Hao, H. C., J. Zhang, and X. Sun, "The deployment of stub structures for mutual coupling reduction in MIMO antenna applications," *Progress In Electromagnetics Research Letters*, Vol. 92, 39–45, 2020.

11. Nguyen, N. L., "Gain enhancement in MIMO antennas using defected ground structure," *Progress In Electromagnetics Research M*, Vol. 87, 127–136, 2019.
12. Sharma, K. and G. P. Pandey, "Two port compact MIMO antenna for ISM band applications," *Progress In Electromagnetics Research C*, Vol. 100, 173–185, 2020.
13. El Ouahabi, M., A. Zakriti, M. Essaaidi, A. Dkiouak, and E. Hanae, "A miniaturized dual-band MIMO antenna with low mutual coupling for wireless applications," *Progress In Electromagnetics Research C*, Vol. 93, 93–101, 2019.
14. Varzakas, P., "Average channel capacity for rayleigh fading spread spectrum MIMO systems," *International Journal of Communication Systems*, Vol. 19, No. 10, 1081–1087, Dec. 2006.
15. Yu, K., X. Liu, and Y. Li, "Mutual coupling reduction of microstrip patch antenna array using modified split ring resonator metamaterial structures," *2017 IEEE International Symposium on Antennas and Propagation & USNC/URSI National Radio Science Meeting*, 2287–2288, San Diego, CA, 2017.
16. Vishvaksean, K. S., K. Mithra, R. Kalaiarasan, and K. S. Raj, "Mutual coupling reduction in microstrip patch antenna arrays using parallel coupled-line resonators," *IEEE Antennas and Wireless Propagation Letters*, Vol. 16, 2146–2149, 2017.
17. Ghosh, J., S. Ghosal, D. Mitra, and S. R. Bhadra Chaudhuri, "Mutual coupling reduction between closely placed microstrip patch antenna using meander line resonator," *Progress In Electromagnetics Research Letters*, Vol. 59, 115–122, 2016.
18. Hwangbo, S., H. Y. Yang, and Y. Yoon, "Mutual coupling reduction using micromachined complementary meander-line slots for a patch array antenna," *IEEE Antennas and Wireless Propagation Letters*, Vol. 16, 1667–1670, 2017.
19. Zhang, J., L. Wang, and W. Zhang, "A novel dual band-notched CPW-fed UWB MIMO antenna with mutual coupling reduction characteristics," *Progress In Electromagnetics Research Letters*, Vol. 90, 21–28, 2020.
20. Gao, D., Z.-X. Cao, S.-D. Fu, X. Quan, and P. Chen, "A novel slot-array defected ground structure for decoupling microstrip antenna array," *IEEE Transactions on Antennas and Propagation*, Vol. 68, No. 10, 7027–7038, Oct. 2020.
21. Ghosh, A., A. Mitra, and S. Das, "Meander line-based low profile RIS with defected ground and its use in patch antenna miniaturization for wireless applications," *Microwave and Optical Technology Letters*, Vol. 59, 732–738, 2017.
22. Chen, Z., M. Tang, Y. Wang, M. Li, and D. Li, "Mutual coupling reduction using planar parasitic resonators for wideband, dual-polarized, high-density patch arrays," *2019 IEEE MTT-S International Wireless Symposium (IWS)*, 1–3, Guangzhou, China, 2019.
23. Cheng, Y., X. Ding, W. Shao, and B. Wang, "Reduction of mutual coupling between patch antennas using a polarization-conversion isolator," *IEEE Antennas and Wireless Propagation Letters*, Vol. 16, 1257–1260, 2017.
24. Addepalli, T. and V. R. Anitha, "A very compact and closely spaced circular shaped UWB MIMO antenna with improved isolation," *AEU — International Journal of Electronics and Communications*, 153016, Vol. 114, Feb. 2020.